International Journal of Engineering & Technology
CENTRE OF PROFESSIONAL RESEARCH PUBLICATIONS
ISSN 2049-3444

International Journal of Engineering and Technology Volume 2 No. 12, December, 2012

Experimental Study of Darcy and Non-Darcy Flow in Porous Media

Oyinkepreye D. Orodu, Favour A. Makinde, Kale B. Orodu
Department of Petroleum Engineering, Covenant University, Canaan Land, Ota, Ogun State, Nigeria

ABSTRACT

A simple experimental set-up is used to validate capillary-tube models of flow in porous media for (non-) spherical particles and coarse grains of particular/specific mesh sizes. Of the two models used, one model characterizes the structure of the media apart from particle diameter or equivalent particle diameter for non-spherical objects compared to the other model. The magnitude of computed tortuosity for particles/grains studied is in order, however, that of the spherical particles was slightly higher than published values for spheres. Likewise, the ratio of dynamic to static specific surface area was below anticipated and known results in literature. For the non-spherical particle that was approximated as a half-oblate spheroid, the possible error in computed volume and surface area may be the reason for the deviation of computed equivalent diameter from the effective diameter obtained by fitting Ergun correlation to experimental result. The deviation of computed results based on the conducted experiment may in fact be due to error in appropriately fitting straight line to plotted data and precision error of gauges, and possible hysteresis at low flow velocity due to experimental procedure.

Keywords: *Darcy, Non-Darcy, Porous media, Ergun, Capillary-tube model*

1. INTRODUCTION

Fluid flow in different media and conduits has gained ground in research over the years by pioneer researchers, and analytical solutions developed. The fundamentals for modeling flow are hinged on the continuity equation, fluid's equation of state and the law governing the dynamics of fluid flow. For flow in a porous media, the constraint in applying a theoretical flow model are characterizing the geometry of the systems of pores, the irregularity of the pore walls that creates fluid converging and diverging, and the interconnected pore system being designated as a bundle of cylindrical tubes. This has necessitated the use of assumptions to simplify the pore system by various researchers in the form of known shape/geometry to obtain analytical and numerical solutions.

Through experimental study, Henri Darcy (1956) established the link between flow rate and pressure gradient in a porous media by a constant of proportionality that is widely referred to as Darcy law. This constant sums up the geometric properties of the porous media. The properties constitute porosity, shape of grains (sphericity and angularity), size of grains, sorting and the degree of cementation (as in subsurface sand grains). That is why correlation for hydraulic conductivity has been established from the first three properties by Sperry and Peirce (1995) and others. A major assumption that is inherent in the development of Darcy's empirical equation is laminar or viscous flow, thereby ignoring inertia forces in the fluid as inherent in the classical Navier-Stokes equation. There exists deviation from the linear relation that is depicted by Darcy's empirical equation (Eqn 1) at high flow rate. This scenario is called non-Darcy flow which occurs at flow rates that is outside the confines of laminar flow regime. For petroleum reservoirs, this phenomenon occurs near the well bore region at the perforation face, gravel pack completions, hydraulic fractured wells (Wu, 2002; Barree and Conway, 2004), and gas reservoirs (Kadi, 1980).

$$v = \frac{k}{\mu}\frac{dP}{dL} \tag{1}$$

where v is superficial velocity; k, permeability; μ, viscosity; L, length of bed or porous media and P, pressure.

Forchheimer (1901) modified the Darcy equation to capture the additional pressure drop observed for high flow rate. However, inertia effects caused by the acceleration and deceleration of flow through the tortuous flow path and not turbulence flow have been attributed to non-Darcy flow. The Forchheimer equation is,

$$\frac{dP}{dx} = \frac{\mu}{k}v + \beta\rho v^2 \tag{2}$$

where ρ is density. The variable "β" in Eqn 2 is called the beta or inertial factor. Other names are non-Darcy and inertial flow coefficient, and turbulence factor. The factor is determined from laboratory test result and multi-rate well tests, and known to be a property of the porous media. By comparing theoretical derivations from different flow models with the Forchheimer equation,

expressions for β (Li and Engler, 2001) had been derived and further extended by empirical correlations to capture pore geometry and the complexity of the pore model. Flow through porous media are commonly modeled by capillary tube (including hydraulic radius models), Navier-Stokes equation, submerged object, statistical, particulate and resistance to flow models for Darcy and non-Darcy flow regimes. The first three models are applicable to non-Darcy flow and the capillary tube models are further subdivided into parallel and serial type models as summarized in Li and Engler (2001). In addition, Barree and Conway (2004) has extended the Forchheimer equation to cover the range beyond which the equation is applicable.

$$\frac{dP}{dL} = 150\frac{(1-\phi)^2\mu}{\phi^3 d^2}v + 1.75\frac{(1-\phi)}{\phi^3 d}\rho v^2 \tag{3}$$

$$\frac{\Delta P}{Hv} = Mv + N = 0.125 f_D \tau^3 a_{vd}\rho\frac{(1-\phi)}{\phi^3}v + 2\gamma\tau^2\mu a_{vd}^2\frac{(1-\phi)^2}{\phi^3} \tag{4}$$

where ϕ is porosity; d, diameter; τ, tortuosity; f_D, Darcy-Weisbach friction factor; γ, shape factor; a_{vd}, ratio of dynamic surface area to volume (dynamic specific surface area) , all other variables as defined in Eqns 1 and 2.

Of particular interest to petroleum engineers on the issue of non-Darcy flow is pressure drop near the well bore region and sand production mitigation with gravel packing or screens with particle entrapment (necessitating anisotropic medium) and its consequences on productivity index as regards to quantifying flow resistance parameters and characterizing the medium with less experimental test and production downtime for multi-rate test. Consequently, the efficacy of the model development from capillary tube having tortuosity and dynamic specific surface area as primary and unknown parameters is verified as a porous media characterizing tool based on a simple experimental setup. Irregular shaped grains of unknown geometric size in terms of surface area and equivalent diameter are tested. In addition, solid sphere and particle of low aspect ratio are also tested.

2. EMPIRICAL MODELS AND APPLICATION

The application of Ergun equation to irregular shaped or non-spherical particles had been based on the replacement of the diameter in the equation by the product of sphericity, a shape factor (Eqn 5) and volume surface mean diameter "d_{vs}" (Eqn 6). This diameter is referred to as Sauter mean diameter in Li and Ma (2011). These authors further compared the use of the commonly applied Sauter mean diameter (Eqn 7) and a product of this diameter with shape factor to hollow spheres and cylinders. Fitting of experimental results gave a better match with the latter (Eqn 8) than that of Sauter mean diameter with the Ergun equation

$$\psi = \frac{A_{sp}}{A_p} \tag{5}$$

$$d_{vs} = \frac{6}{\left(A_{sp}/V_p\right)} \tag{6}$$

$$d_{sd} = \frac{6}{\left(A_p/V_p\right)} = \psi d_{vs} \tag{7}$$

$$d_{eq} = \psi d_{sd} \tag{8}$$

where A_p is surface area of particle; A_{sp}, surface area of the equivalent-volume sphere; d_{eq}, equivalent diameter of non-spherical particles; d_{sd}, Sauer mean diameter; d_{vs}, volume-surface mean diameter; and ψ, Wadell's sphericity.

For Eqn 4, the Comiti and Renaud equation, dynamic specific surface area "a_{vd}" is equal to the term in brackets of Eqn 7 for spherical particles. However, for other shapes the ratio is less than 1.0. "M" and "N" (Eqns 4, 9 and 10) are the gradient and intercept of the straight line plot from experimental data to compute constants that characterize the porous media. Darcy-Weisbach friction factor (f_D) is the popular correlation used for pressure drop computation due to flow resistance from the pipe walls. Use of friction factor equation for laminar flow reduces

Nonetheless the Forchheimer equation can be used to determine permeability of a medium based on experimental data, empirical correlations like that of the commonly applied Ergun equation (1952) which is widely used for spherical particles and irregular particles with readily obtainable equivalent pore diameter or not. The Ergun equation and other empirical equations are capable of characterizing the porous media with properties such as particle diameter and porosity for Ergun equation and that of Comiti and Renard (1989) for porosity, tortuosity, and dynamic specific surface area. For spherical object, the dynamic specific surface area collapses to a form of the hydraulic radius. While Ergun equation former correlation focuses on particle characterization, the other adds on the flow medium.

Eqn 4 to 11 which is related to the Darcy equation, and adapts the use of turbulent flow friction, in particular, Nikuradse's friction factor correlation (Eqn 12) for turbulent flow in rough pipes. Solutions of Eqns 9 and 10 give expressions for tortuosity and dynamic specific surface area, Eqn 13 and Eqn 14, while Eqn 15 and 16 are based on the modification of Eqn 4 for wall effect and can be solved by optimization of the respective equations.

$$N = 2\gamma\tau^2\mu a_{vd}^2\frac{(1-\phi)^2}{\phi^3} \tag{9}$$

$$M = 0.125 f_D \tau^3 a_{vd}\rho\frac{(1-\phi)}{\phi^3} \tag{10}$$

$$\frac{\Delta P}{H} = \left(0.125\left(\frac{64\mu}{\rho d}\right)\tau^3 a_{vd}\rho\frac{(1-\phi)}{\phi^3} + 2\gamma\tau^2\mu a_{vd}^2\frac{(1-\phi)^2}{\phi^3}\right)U_o \tag{11}$$

$$\frac{1}{\sqrt{f_D}} = 1.75 - 2\log_{10}\left(\frac{2e}{D}\right) \tag{12}$$

$$\tau = \left[\frac{M^2}{N}\frac{2\gamma\mu\phi^3}{(0.125 f_D\rho)^2}\right]^{1/4} \tag{13}$$

$$a_{vd} = \left[\frac{N^3}{M^2}\frac{(0.125 f_D\rho)^2}{(2\gamma\mu)^3}\frac{\phi^3}{(1-\phi)^4}\right]^{1/4} \tag{14}$$

$$\left\{\left(1-0.125 f_{DW}\left(1-\frac{d_p}{D}\right)^2\right)+0.125 f_D\left(1-\frac{d_p}{D}\right)^2\right\}\left(\frac{\tau^2\rho}{\dot{M}}\left(\frac{N}{2\varepsilon^3\mu\gamma}\right)^{\frac{1}{2}} - \frac{4\tau^3\rho}{D\dot{M}\varepsilon^3}\right) - 1 = 0 \tag{15}$$

$$\frac{1}{D}\left(\frac{2\mu\gamma}{\dot{N}\varepsilon}\right)^{\frac{1}{2}}\left(\frac{\dot{M}}{\rho(1-\varepsilon)\left\{\left(1-0.125 f_{DW}\left(1-\frac{d_p}{D}\right)^2\right)+0.125 f_D\left(1-\frac{d_p}{D}\right)^2\right\}}\right)^{\frac{1}{3}}\left\{a_{vd}(1-\varepsilon)+4\right\} - a_{vd}^{\frac{1}{3}} = 0 \tag{16}$$

3. DESCRIPTION OF EXPERIMENT

3.1 Sieve Analysis of Aggregates/Gravel

In order to obtain an unconsolidated porous media, sieve analysis is carried out. Sieve analysis helps to determine the particle size distribution of the coarse and fine aggregates. This is done by sieving the aggregate based on the standard of the IS code. The aggregates pass through the different layers of sieves with respect to the mesh size in order to obtain the corresponding size particles.

3.2 Porous Media Particles

Particles (Table 1) that make up the porous media for investigation in this study are presented in Fig 1a-f. Figures 1c-f which are the outcomes of sieving described in the previous subsection for gravel. The Non-Spherical beads of Fig. 1b are disked-shaped beads called sequins whose volume and surface area are computed based on the half oblate spheroid shape of 2.3×2.65mm. Table 2 shows the measured data and computed parameters of the spheroid. Volume and surface area of the sequin is calculated by Eqns 17 and 18.

$$V = \frac{4}{3}\pi a^2 b \tag{17}$$

$$s = 2\pi a^2\left(1+\frac{1-e^2}{e}\tanh^{-1}e\right) \tag{18}$$

where all the parameters are as defined in Table 2 and below.

$$e^2 = 1-\frac{b^2}{a^2}$$

(a) **(b)** **(c)**

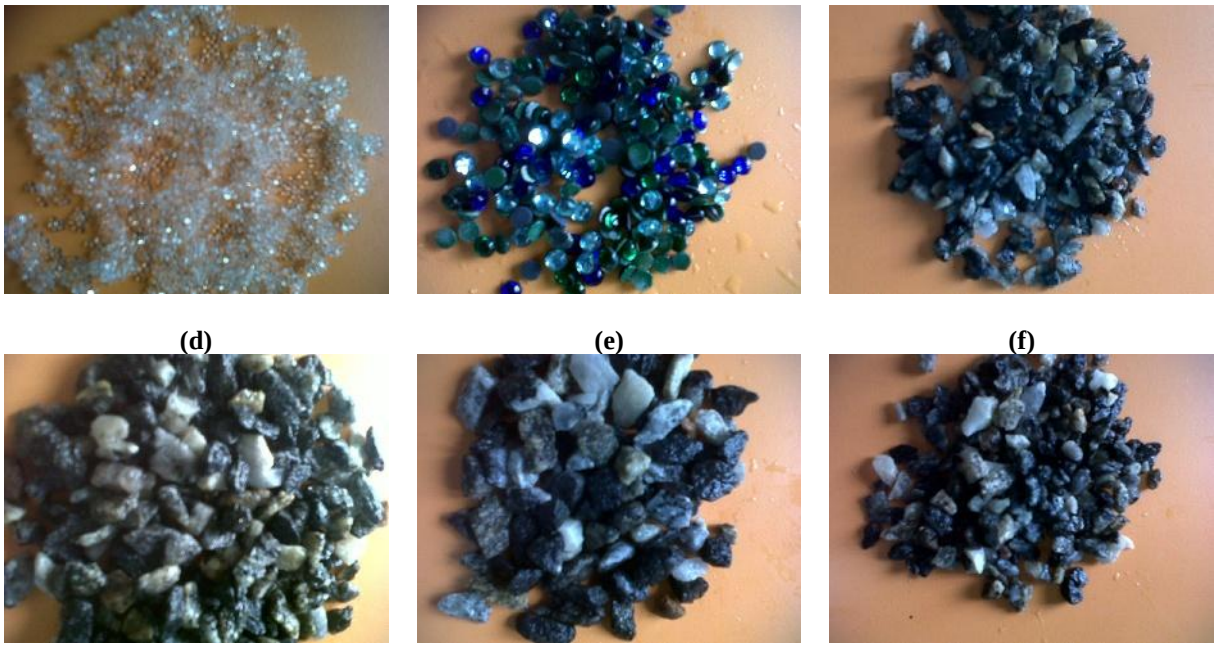

Fig. 1. (a) Ballotini - 1mm spherical glass beads (b) Non-Spherical beads – Oblate Spheroid of 2.3×2.65mm (c) 4.75mm US standard mesh size gravel (d) 6.3mm US standard mesh size gravel (e) 9.5mm US standard mesh size gravel and (f) 4.75 + 6.3mm US standard mesh size gravel mixture representing highly anisotropic porous media.

Table 1: Particles for experiment

Particle	ε	Diameter (mm)
Spherical Bead (Ballotini)	0.380	1.0
Non-Spherical Bead (Sequin)	0.401	-
Gravel 4.75mm	0.495	-
Gravel 6.3mm	0.523	-
Gravel 9.5mm	0.594	-
Gravel 4.75+6.3mm	0.520	-

Table 2: Computed and measured data of non-Spherical Bead

Parameter	Value
a, semi-major axis	2.65mm
b, semi-minor axis	2.3mm
V, particle volume	$3.38281e^{-8}$ m^3
A_p, particle surface area	$6.23559e^{-5}$ m^2
A_{sp}, surface area of equivalent-volume sphere	$5.05828e^{-5}m^2$
d_{vs}, volume-surface mean diameter	4.013mm
ψ, Wadell's sphericity	0.811
d_{sd}, Sauter mean diameter	3.255mm
d_{eq}, equivalent diameter of non-spherical particle	2.640mm
f, oblatness or flattening	0.132

3.3 Flow Equipment

The equipment line-up is made up of a vertical Perspex column 38mm internal diameter and 500mm long with inlet and outlet connections for water flow in both directions (Fig. 2). Granular media is retained within the column by a 0.5mm gauze mesh (B.S. 30 sieve mesh) at the base. Water source is through a constant head tank of 8.3 liters capacity at 2.5m above the column that is fitted with an overflow weir for constant water level. Flow rate range is 50-800 cm^3/min by the aid of a variable flow device as given by the top edge of a float. The top and bottom of the column is connected to the top and bottom of a manifold block. Water from the top and bottom of the column are isolated in the manifold whose ends are connected to a U-tube water and mercury manometer. The water manometer is used in the experiment for this study for safety. The ends of the water manometer are linked at the top and which allows air pressure to be adjusted. The setup enables easy removal of trapped air through drain valves, bleed screw at the connecting end of the water manometer and top of the column. The commissioning process ensures this.

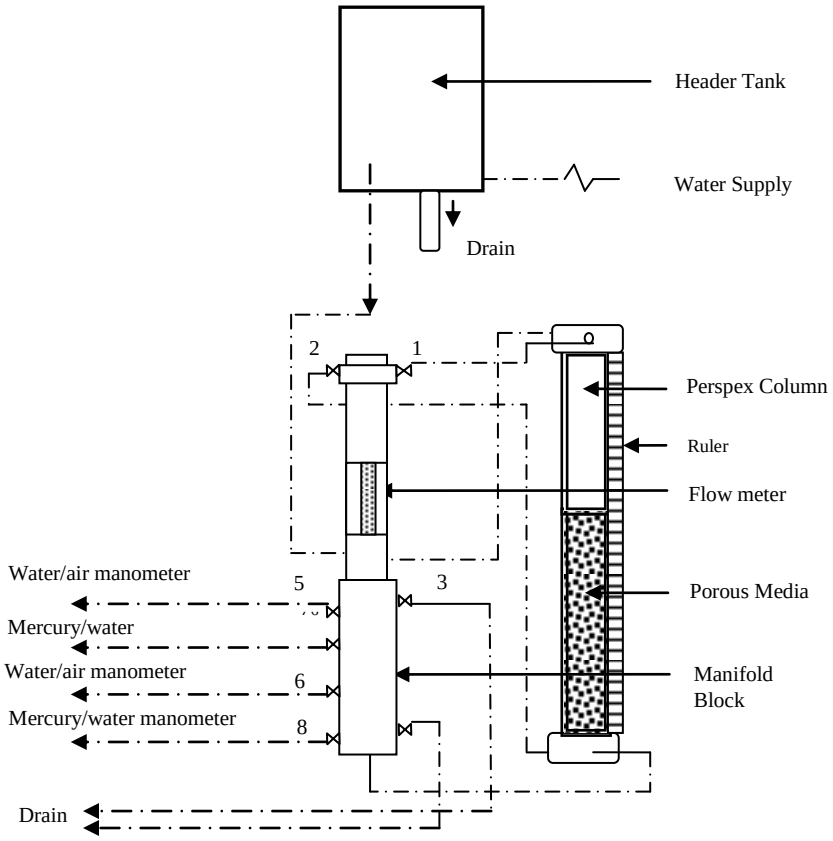

Fig. 2: Experimental setup

3.4 Quality of Measurement

For each porous media, water head is measured at increase of flow from 100-800cm^3/min and flow decrease back to 100cm^3/min and eventually to zero to establish consistency in readings. However, significant difference occurred (was observed) at low flow rate. At each flow rate, steady state was ensured by allowing flow for a few minutes. The laid down commissioning process of the equipment was carried out and air bubbles in the flow tubes and porous media that could affect reading was avoided. The accuracy of the test shall be tested for a solid sphere (Ballotini) as the porous medium with the established Ergun equation.

Systematic and random errors are possible. The former is on the precision of the water U-tube manometer, and to a lesser extent on flow measuring device. Other errors are systematic in obtaining flow rate from the scale by observing the float level and water manometer height.

Porosity for each test bed particle was obtained by bulk volume measurement in the graduated test bed column and particle volume through water displacement in a graduated measuring cylinder. The particles were removed from the test bed to obtain the volume. Measurement of bulk volume in the test bed was for accuracy due to possible change in sorting and orientation of particles for non-spherical particles and grains with respect to angularity and sphericity, and structure for the disk like particle.

4. RESULTS AND DISCUSSION

Figure 3.1 shows the superiority of the correlation obtained from the regression as shown in Figure 3.2. The regression equation clearly shows a higher representation/model for the experimental data, however, Figure 3.3 depicts the fact the Ergun correlation is quite a reasonable fit for the experiment. In addition, the MSE and RMSE for the Ergun Equation and obtained correlation are 0.025 and 0.01 for MSE, 0.159 and 0.098 for RMSE respectively. Reasons for the deviation from Ergun correlation lie in the fact that as stated by Cheng (2011), the equation is applicable for no wall effect on flow with respect to the ratio of flow tube diameter to sphere diameter being greater than 40. However, Ergun (1952) had alluded to the fact that the ratio being less than 10 showed scatter from the trend by the Ergun equation.

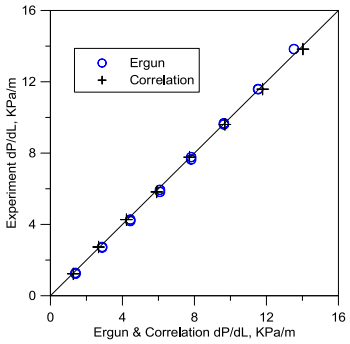

Fig 3.1. Plot of experimental data against estimation by Ergun's equation and developed correlation for Spherical Bead

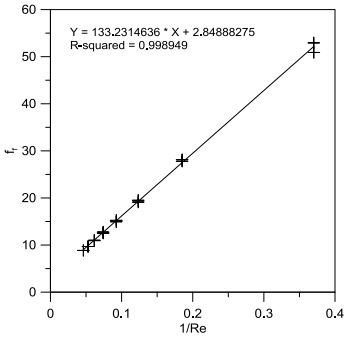

Fig 3.2. Plot of friction factor against pore Reynolds number, for Spherical Bead

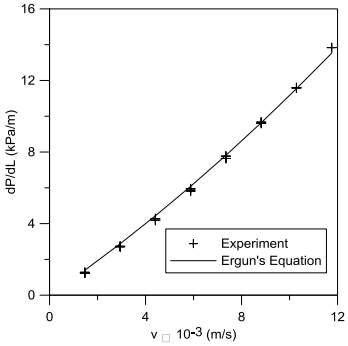

Fig 3.3. Plot of pressure drop against superficial velocity based on Ergun's equation and experimental data, for Spherical Bead.

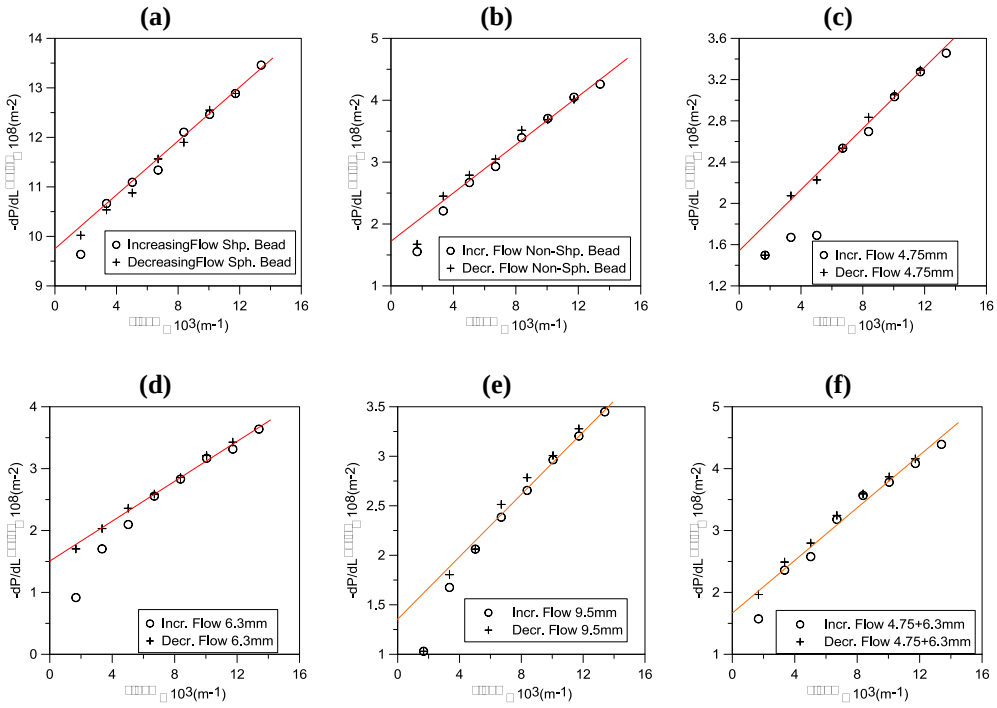

Fig. 4: Forchhheimer's experimental linear plot fitting of $-dP/[dL\times(V_s\mu)^{-1}]$ against $\rho V_s/\mu$(a) Ballotini - 1mm spherical glass beads (b) Non-Spherical beads – Oblate Spheroid of 2.3×2.65mm (c) 4.75mm US standard mesh size gravel (d) 6.3mm US standard mesh size gravel (e) 9.5mm US standard mesh size gravel and (f) 4.75 + 6.3mm US standard mesh size gravel mixture representing highly anisotropic porous media.

Flow regime in porous media has been classified based on a function of pressure gradient into Pre-Darcy, Darcy and Non-Darcy flow by plotting superficial velocity against pressure gradient and observing the linear trend that passes through the origin of the graph when extended as it denotes the Darcy flow region. While the Pre-Darcy starts before Darcy flow, and that of Non-Darcy is after the Darcy flow regime. This is the first step at analyzing the experimental data obtained for different porous media (packing) in a constant diameter column. The Perspex column filled with 1mm spherical glass beads had about 75% of data points within the Darcy flow region and the others, non-Darcy flow region, while the other packing materials from non-Spherical Beads (≈oblate spheroid) to different sized gravels from US standard mesh dimension of 4.7mm, 6.3mm and 9.5mm all have about 90% of data points within the Non-Darcy flow region.

At low flow rate or superficial velocity, the deviation of data points from the obvious straight trend seems uniform from the spherical bead to non-spherical bead packing and to the gravel packing (this differences hovers around

0.5×10^8 inverse apparent permeability units). The logical deviation of data point either from the straight line trend or between that of decreasing and increasing flow rate may be explained logically from the effect of initial unsteady state flow that is brought about by the dominance of viscous flow. Or the trend may be explained by uniform velocity distribution at higher velocity than low velocity as flow is not subjected to only larger pores as in low velocity (Barree and Conway (2004)). This trend is not observed in the previous plot of superficial velocity against pressure gradient. In similar manner, the match of experimental results for laminar flow (low velocity) was less than that for higher velocity as observed by Li and Ma (2011). It is worth mentioning that the Ergun-equation is a superimposition of laminar and turbulent flow in tubes as related to flow in porous (Bird *et a.l*, 2002), hence, the equation reduces to laminar flow at low velocity and so would not be like a correlation/equation developed for only laminar flow.

Table 3: Sauter diameter and equivalent diameter modification due to uncertainty of volume and total surface area.

		A_p 0%	A_p-10%	A_p-20%	A_p-30%
V 0%	d_{sd} (mm)	3.255	3.374	3.503	3.642
	d_{eq} (mm)	2.640	2.836	3.058	3.331
V -10%	d_{sd} (mm)	2.930	3.037	3.153	3.277
	d_{eq} (mm)	2.215	2.381	2.565	2.773
V -20%	d_{sd} (mm)	2.604	2.270	2.802	2.913
	d_{eq} (mm)	1.820	1.960	2.108	2.278
V -30%	d_{sd} (mm)	2.279	2.362	2.452	2.549
	d_{eq} (mm)	1.457	1.566	1.688	1.824

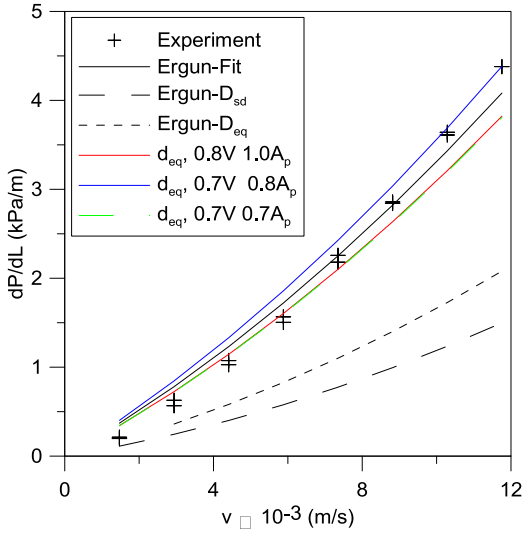

Fig. 5: Pressure gradient correlation by Ergun's equation for experimental data fitted to Ergun's equation, computed equivalent diameter and diameter modified with respect to uncertainty of non-spherical particle's volume and surface area.

For the non-spherical object of Fig 1b, the object shape is approximated to a half-oblate spheroid. This of course should have some implications on computing volume and surface area, which is the reason for the approximation. Measured data/readings and computed values are tabulated as seen in Table 2.

Sauter and equivalent diameter obtained from approximation of the non-spherical particle by half-oblate spheroid is used to compute pressure gradient based on the Ergun's equation. Other computation is based on fitting the Ergun's equation to the experimental data and uncertainty associated with the particle's volume and total surface area. Table 3 shows the range of uncertainty and Figure 5 shows the deviation of the computed values from the experimental result. The uncertainty in volume and surface area indicated by decrease of (20%, 0%), (30%, 20%) and (30%, 30%) in volume and surface area gave a closer fit to the experimental result. An effective diameter for the experimental set-up is 1.75mm. Whatever error that may lie in the volume and surface area as represented by the oblate spheroid and can be as high as 20-30% by inference from the shape of the particle. Hence, irregular shaped objects may be faced with the issue of computing volume and surface area, as such, reliance on fitting experimental results. However, the orientation of the particles being random and layer-like in some spots may contribute to deviation from Ergun-equation, another equally possibility is the ratio of the column to equivalent particle diameter.

The equation Eqn 4 was developed to model fluid (liquid) flow in a porous media based on the media being represented by a bundle of tubes, or better expressed as being equivalent to a single tube with a diameter (Comiti and Renaud, 1989). The model entails the sum of creeping (laminar) and turbulent (inertial) flow regimes that signifies viscous resistance at pore walls and inertial resistance of kinetic energy loss by change in flow direction. Pressure drop due to friction was applied to compute kinetic energy loss. In particular, Nikuradse's friction factor correlation was applied. Though not explained, this carefully avoids the use of velocity and its application avoided the direct use of diameter and absolute roughness. In applying the computed equivalent

diameter and velocity of pipe flow, the flow regime is a laminar flow. On using the theoretical expression for computation of friction factor in the equation for non-Darcy flow in a porous media as represented by the kinetic energy loss of inertia and viscous flow, the equation reduces to a Darcy flow expression thereby not capturing non-Darcy flow. The reduced equation is shown in Eqn 11. However, Ma and Ruth (1997) argue that for straight tube model, non-Darcy flow effects will not become existent until true turbulence sets in at Re≈2000, while in a bent tube model, microscopic inertial effects will become important when Re≈1. So the importance of tortuosity and the likely and unexplained reason for the use of turbulent flow friction factor correlation by Comiti and Renaud, (1989). In contradiction, Li and Engler (2001) reported that Bear (1972), Scheidegger (1974), Barak (1987) and Ruth and Ma(1992) agreed that nonlinearity between pressure gradient and velocity is not due to turbulent flow in porous media but to inertial effects.

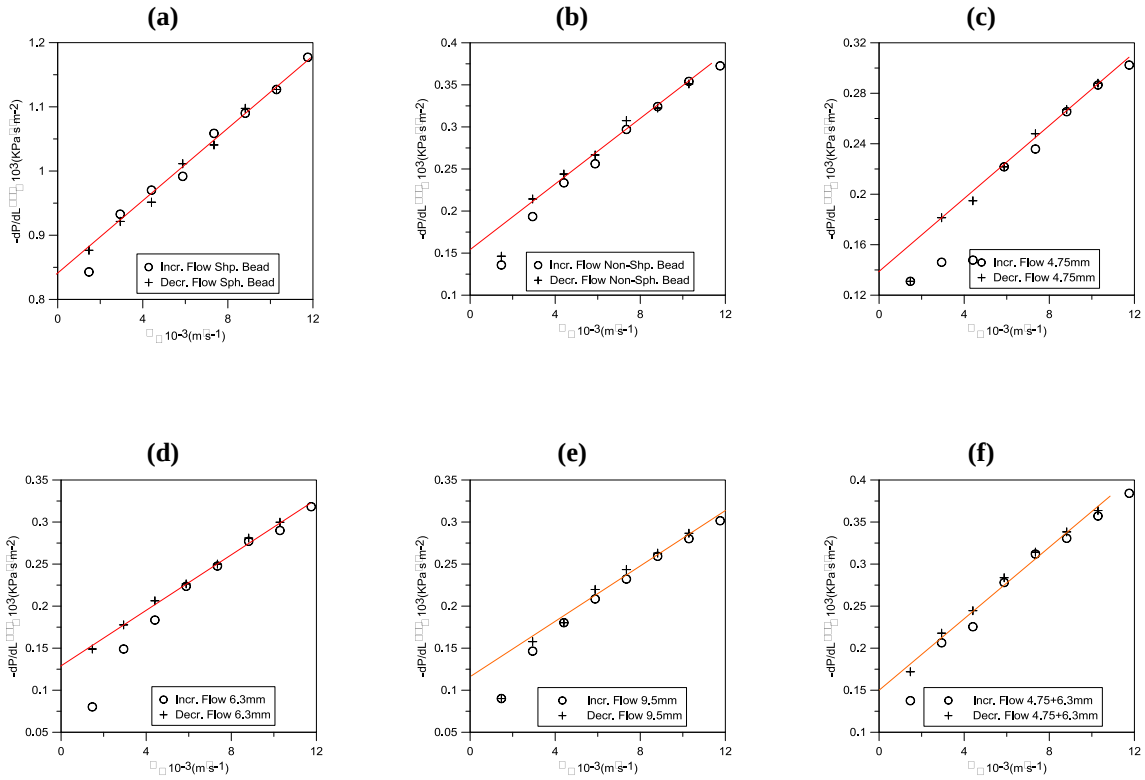

Fig. 6: Comiti and Renard experimental linear plot fitting of $-dP/[dL\times(V_s)^{-1}]$ against V_s (a) Ballotini - 1mm spherical glass beads (b) Non-Spherical beads – Oblate Spheroid of 2.3×2.65mm (c) 4.75mm US standard mesh size gravel (d) 6.3mm US standard mesh size gravel (e) 9.5mm US standard mesh size gravel and (f) 4.75 + 6.3mm US standard mesh size gravel mixture representing highly anisotropic porous media.

Forchheimer and Comiti and Renaud (1989) plots (Fig. 4 and 6) are similar, the former plot is $[-\Delta P/(\Delta L\cdot v\cdot\mu)]$ against $[\rho\cdot v/\mu]$ to obtain permeability as is commonly applied while the later authors plot $[-\Delta P/(\Delta L\cdot v)]$ against $[v]$. The difference arises in the constants of viscosity and density which for an incompressible flow is inconsequential. However, for compressible flow, it is not. In relation to Ergun's equation (Ergun and Orning, 1949), this equation and that of Comiti and Renaud were shown as been derived from the Poiseuille equation for the viscous term and kinetic energy loss in pipe flow for the inertial term for the pressure gradient in a porous media. The difference of the former is the capability to capture and model flow of packed media of parallelepipedal particles, or particles having very low height to side ratio by the introduction of a parameter that considers the dynamic surface area in contact with the fluid during flow which is also linked or connected to the orientation of the particles. In addition, the equation is applicable in considering wall effect while the higher difference in plotted data at low flow velocity between readings taken at increasing and decreasing flow may be attributed to hysteresis.

Table 4: Intercept, slope and structure parameters of Equation 4 for all media

Particle	ε	$M\times10^{9}$ $Pa\cdot s^{2}\cdot m^{-3}$	$N\times10^{6}$ $Pa\cdot s\cdot m^{-2}$	d_{eq} mm	τ	a_{vd} m^{-1}	a_{vs} m^{-1}	X
Spherical Bead	0.380	0.028311	0.83990	1.00	1.789	4627	6000	0.77
Non-Spherical Bead	0.401	0.019553	0.15330	1.84	2.364	1670	3260	0.51
4.75mm Gravel	0.495	0.021323	0.14905	1.27	2.440	2521	4720	0.53
6.3mm Gravel	0.523	0.014423	0.13923	1.09	2.762	2427	5510	0.44
9.5mm Gravel	0.594	0.016507	0.12880	0.89	3.150	2903	6750	0.43
4.75+6.3mm Gravel	0.520	0.016616	0.11500	1.00	3.030	2383	5999	0.40

Equation 4 gives expressions for tortuosity, "τ" and a_{vd} (dynamic specific surface area or ration of surface area presented by the particles to the flow to volume of solid) of the porous media in the form of Eqns 13 and 14. The corresponding parameters of M, N, τ, a_{vd}, a_{vs} and X for the porous media as shown in Fig 1 are presented in Table 4. Apart from the spherical beads, the a_{vs} of the other porous media were calculated from equivalent diameter based on Ergun's correlation (as in Ergun-Fit in Fig. 5 for the sequin bead) due to the irregular shape. It is obvious that the spherical bead has the largest dynamic contact surface area. The low contact area and high tortuosity for the gravels of various mesh size with respect to the spherical bead may be largely due to sphericity, angularity and heterogeneity. Equation 4 consists of parameters that are defined and accounts for the structure of the porous media for characterizing it unlike numerical constants in Erguns' equation without a physical meaning. Verification of parameters in the form of tortuosity and dynamic surface area had been shown in literature; however, Kozeny and Carmen equation had shown the value of tortuosity and its relevance for the porous media.

The study of wall effect on flow and pressure gradient may not be properly defined for irregular objects. Equivalent diameter based on fitting of experimental data should distort the application of the modified Eqn 4 gradient and intercept to Eqns 15 and 16 for wall effect. Wall effect accounts for computation of friction on the wall face and inertia contribution to pressure gradient.

5. CONCLUSIONS

- The effective particle diameter obtained by fitting experimental data with the Ergun equation is different from that of the computed equivalent diameter for the non-spherical bead (disk-like sequin). With the approximation of the sequin as a semi-oblate spheroid, equivalent diameter was computed. However, based on the assumption of error in calculated volume and surface area due to this approximation, the percentage error was obtained.

- For spherical shaped particles, static specific surface area 'a_{vs}' is equal to dynamic specific surface area 'a_{vd}'. This was not achieved for the Ballotini (spherical) beads. As such, the ratio of 'a_{vd}' to 'a_{vs}' was less than 1.0. A value of 0.77 was computed, however, that of the non-spherical particles were much less than that of the spherical bead as expected. This indicates less fluid contact area with the particles.

- Tortuosity for spheres had being noted to have a value of about 1.44 according to various studies. The value computed for the spherical bead in this study was 1.789, while that of the non-spherical particles was higher as expected.

- Attempt was made to apply the published model of Comiti and Renard that was modified for wall effects. The application of the model required the optimization of the derived equations to obtain tortuosity and dynamic specific surface area. Non-unique solutions were obtained.

REFERENCES

[1] Barak, A. Z. 1987. Comments on High Velocity Flow in Porous Media by Hassanizadeh and Gray, Transport in Porous Media, 1(1987):63-97.

[2] Barree, R. D., Conway, M. W. 2004. Beyond Beta Factors: A Complete Model for Darcy, Forchheimer, and trans-Forchheimer Flow in Porous Media, SPE Paper 89325 presented at the SPE Annual Technical Conference and Exhibition, Houston, Texas, USA, 26-29 September.

[3] Bear, J. 1972. Dynamics of Fluids in Porous Media, Dover Publications, Inc., New York.

[4] Bird, R. B., Stewart, W. E., Lightfoot, E. N. 2002. Transport Phenomena, 2nd ed., John Wiley & Sons, pp188-191.

[5] Cheng, N. 2011. Wall Effect on Pressure Drop in Packed Beds, Powder Technology, 210(3): 261—266.

[6] Comiti, J, Renaud, M. 1989. A New Model for Determining Mean Structure Parameters of Fixed Beds from Pressure Drop Measurements: Application to Beds Packed with Parallelepipedal Particles, Chemical Engineering Science, 44(7): 1539-1545.

[7] Ergun, S. 1952. Fluid Flow through Packed Columns, Chemical Engineering Progress, 48(2): 89-94.

[8] Ergun, S., Orning, A. A. 1949. Fluid Flow through Randomly Packed Columns and Fluidized Beds, Industrial and Engineering Chemistry, 41(6): 1179-1184.

[9] Forcheimer, P. 1901. Wasserbewegung durch boden, Z. Ver. Deutsch. Ing. 45.

[10] Kadi, K. S. 1980. Non-Darcy Flow in Dissolved Gas—Drive Reservoir, SPE paper 9301, 55th SPE Annual Fakll Tech. Conference, Dallas.

[11] Li, D., Engler, T. W. 2001. Literature Review on Correlations of the Non-Darcy Coefficient, SPE Paper 70015 presented at the SPE Permian Basin oil and Gas Recovery Conference, Midland, Texas, USA, 15-26 May.

[12] Li, L., Ma, W. 2011. Experimental Study on the Effective particle Diameter of a Packed Bed with Non-Spherical Particles, Transport in Porous Media, 89(1): 35-48

[13] Ma, H., Ruth, D. 1997. Physical Explanations of Non-Darcy Effects for Fluid Flow in Porous Mdeia, SPE Formation Evaluation, (March): 13-18.

[14] Ruth, D., Ma, H. 1992. On the Derivation of the Forchheimer Equation by Means of the Average Theorem, Transport in Porous Media, 7(3): 255-264.

[15] Scheidegger, A. E. 1972. The Physics of Flow through Porous Media, University of Toronto Press, Toronto.

[16] Sperry. J. M., Peirce, J. J. 1995. A Model for Estimating the Hydraulic Conductivity of Granular Material Based on Grain Shape, Grain Size, and Porosity, Ground Water, 33(6): 892-898.

[17] Wu, Y. 2002. An Approximate Analytical Solution for Non-Darcy Flow Toward a Well in Fractured Media, Water Resources Research 38(3): 1023.

